A01-34528

AIAA-2001-3898

Performance Study of the Ablative Z-pinch Pulsed Plasma Thruster

Michael Keidar, Iain D. Boyd and Neal Lepsetz

University of Michigan, Ann Arbor MI 48109

Thomas E. Markusic, Kurt A. Polzin and Edgar. Y. Choueiri

Princeton University, Princeton NJ 08544

37th AIAA/ASME/SAE/ASEE Joint Propulsion Conference and Exhibit

8-11 July 2001
Salt Lake City, Utah

AIAA –2001-3898

Performance Study of the Ablative Z-pinch Pulsed Plasma Thruster

Michael Keidar[♦], Iain D. Boyd[*] and Neal Lepsetz[♣]

Department of Aerospace Engineering, University of Michigan, Ann Arbor, MI 48109

Thomas E. Markusic[♥], Kurt A. Polzin[♥], and Edgar Y. Choueiri[♠]

Electric Propulsion and Plasma Dynamic Laboratory (EPPDyL), Princeton University, Princeton, NJ 08544

Abstract

The ablative Z-pinch PPT utilizes the Z-pinch effect to produce an axially streaming plasma. When the current is fully pinched in this device, a large axial pressure gradient exists and thus plasma accelerates in the axial direction due to the gasdynamic force. In the present paper, a model of the electrical discharge in the Ablative Z-pinch Pulsed Plasma Thruster is developed. The model includes Joule heating of the plasma, heat transfer to the Teflon, and Teflon ablation. Mechanisms of energy transfer from the plasma column to the propellant include heat transfer by particle convection and by radiation. The computation of Teflon ablation is based on a recently developed kinetic ablation model. The average current density in the pinched region is used as a parameter of the model. The model predicts that the electron temperature peaks at about 4 eV and the plasma density peaks at about $8 \cdot 10^{23}$ m^{-3}. Thruster performance characteristics such as impulse bit, specific impulse and the mass bit are calculated. In the case of low pulse energy, all measured thruster performance characteristics agree with our model predictions when the average current density to the anode current density ratio α is about 0.55. In the case of high pulse energy, such an agreement with the experiment occurs when $\alpha \approx 0.7\text{-}0.8$, that suggests that in the case of higher pulse energy the current is more constricted near the anode tip. The model also predicts that the impulse bit decreases with increasing propellant inner diameter in agreement with experiment. The comparison of the model prediction with experimental data suggests that the pinch effect and the thrust-to-power ratio increase with the pulse energy.

♦ *Research Scientist, Department of Aerospace Engineering, Member of AIAA*
* *Associate Professor, Department of Aerospace Engineering, Senior Member of AIAA*
♣ *Undergraduate student, Department of Aerospace Engineering*
♥ *Graduate student*
♠ *Chief Scientist at EPPDyL. Assistant Professor, Applied Physics Group, Senior Member AIAA*

1. Introduction

Due to the combined advantages of system simplicity, high reliability, low average electric power requirement and high specific impulse, currently there is a renewed interest in pulsed plasma thrusters (PPT's) for a number of missions[1]. The PPT is considered as an attractive propulsion option for orbit insertion, constellation maintenance, drag makeup and attitude control of small satellites. Existing PPT's, however, have very poor performance characteristics with an efficiency[2] at the level of about 10% that leaves an opportunity for substantial improvement.

To improve the PPT performance, several directions are being considered, such as elimination of late-time ablation, choice of the proper current waveform etc[3]. Currently, new PPT devices using both an electromagnetic acceleration mechanism[4,5] or an electrothermal mechanism are under development[6,7]. One of the motivations for development of new PPT configurations is to achieve higher thrust-to-power ratio. Electrothermal PPTs that were developed by Burton at. al.[6,7] have thrust-to-power ratio >35 μN/W. Another approach for producing a high thrust-to-power PPT involves using the inverse Z-pinch effect, as demonstrated by Mikellides and Turchi et. al.[8].

Z-pinch plasmas produced by the magnetic compression of a cylindrical plasma column are used widely to produce hot and dense plasmas for many applications that include focusing of energetic particles, guiding intense optical laser pulses, and producing ultrahigh magnetic fields. While the macroscopic dynamics of the Z-pinch plasma can be described in terms of snowplow model the details of the current structure and other plasma properties are not completely understood[9]. The idea to use the Z-pinch geometry for a plasma thruster was first proposed by Jahn et. al[10]. Recently some interesting results on the application of the Z-pinch configuration for an ablative Pulsed Plasma Thruster were presented[11]. The Ablative Z-pinch PPT utilizes the pinch

effect to produce axially streaming plasma. It was found that a specific impulse of about 809 s, a thrust-to-power ratio of about 27.8 μN/W and a thrust efficiency of 8.95% were the highest performance values obtained for the best current AZ-PPT designs. When the current is fully pinched in this device, a large axial pressure gradient exists and thus the plasma accelerates in the axial direction. Therefore, the main mechanism of plasma acceleration is electrothermal due to the gasdynamic force. This motivates us to use a previously developed model for electrothermal PPT's to describe the Z-pinch PPT.

Another interesting effect that may enhance the AZ-PPT performances is the plasma macroparticle interactions. Macroparticles are large chunks (1-100 μm diameter) of the Teflon that are emitted during the pulse. Estimates have shown that the particulate emission consumes about 40% of the total propellant mass, while contributing only 1% to the total thrust[12]. Specific design of the AZ PPT allows the discharge chamber to act as a macroparticle trap as was mentioned in Ref. 11. Previously we showed that the macroparticle interaction with a discharge plasma may lead to complete decomposition of some macroparticles[13]. For instance, it was found[13] that a 5 μm diameter macroparticle would completely decompose during the 10 μs of the interaction with a plasma under typical conditions of an electrothermal PPT. Therefore macroparticle trapping can increase the time spent by the macroparticle in the discharge that will lead to increased macroparticle ablation and thus better propellant utilization.

In this paper, we describe the model of the electrical discharge in the AZ-PPT. Knowing the plasma parameter evolution during the pulse allows us to calculate the performance characteristics of the thruster such as specific impulse, impulse bit and mass bit. The present work is based on a previously developed model of the ablation controlled discharge[14,15]. This model was successfully used to model elecrtrothermal PPT's developed at the University of Illinois[6,7]

(PPT-4, PPT-7). The model includes Joule heating of the plasma, heat transfer to the Teflon, and Teflon ablation. Mechanisms of energy transfer from the plasma column to the propellant bar include heat transfer by particle convection and by radiation. The computation of Teflon ablation is based on a recently developed kinetic ablation model[16].

In the following section we will describe the model in brief that includes both sheath and quasi-neutral plasma as well as plasma-dielectric interaction.

2. The discharge model

The model considers the plasma generation processes (ablation, heating, radiation, ionization etc.) and plasma acceleration along a Teflon chamber. Some characteristic regions such as the Teflon surface, electrical sheath near the dielectric and quasi-neutral plasma are shown in Fig. 1. Different kinetic and hydrodynamic phenomena determine the main features of the plasma flow including plasma Joule heating, heat transfer to the dielectric and electrothermal acceleration of the plasma up to the sound speed at the cavity exit. Below, we will discuss the model in the different regions and the full system of equations including the final expressions obtained previously [15]. In addition, we will estimate the current distribution in the pinched area in order to obtain the current density that will be used in the energy balance.

Firstly, let us estimate the characteristic time for the pinch effect. In the frame of the simple snowplow model when the current rise is linear, it was shown that the time constant for pinch[17]:

$$\tau = (\mu\rho)^{1/4} L/(dI/dt)^2$$

where μ is the permittivity, ρ is the initial plasma density, dI/dt is the current rise, and L is the characteristic initial size. For the range of parameters typical for an AZ-PPT, an estimation shows that the current pinch time is $<10^{-7}$ s. This means that after that time, the current is strongly pinched. This statement is certainly supported by the experimental observations presented earlier [11]. Therefore, in our model, we have assumed that during the discharge (~10 μs) the current is fully pinched.

2.1. Electrostatic Sheath

According to our previous estimations[15] during the discharge pulse, a quasi-steady sheath structure is formed and that under typical PPT conditions, this sheath is unmagnetized (the self-magnetic field generated during the pulse is considered). In this case, the potential drop of the electrostatic sheath near the Teflon wall, is negative in order to repel the excess of the thermal electrons, so that the random electron current density j_{eth} is equal to the Bohm ion current density j_i. Under these conditions the potential drop in the sheath can be calculated as:

$$U_d = -T_e \ln (j_{eth}/j_i) \quad \text{.....(1)}$$

2.2. Teflon ablation

In the present work the Teflon ablation is modeled in the framework of the approximation[18] based on a previously developed kinetic model of metal evaporation in a surrounding plasma[19]. The mathematical description includes the model for two different layers between the surface and the plasma bulk: (1) a kinetic non-equilibrium layer adjusted to the surface with a thickness of about one mean free path; and (2) a collision-dominated layer with thermal and ionization non-

equilibrium. The plasma-wall transition layer also includes an electrical sheath described in the previous section. This model makes it possible to calculate the plasma parameters (density and temperature) at the interface between the kinetic and hydrodynamic layers. For known velocity and density at this interface, it is possible to calculate the ablation rate. The ablation rate is formulated according to Ref. 16 as follows:

$$\Gamma = mV_1n_1 = n_1[(2kT_1/m)\cdot(T_2n_2/2T_1 - n_1/2)/(n_1 - n_1^2/n_2)]^{0.5} \quad (2)$$

where n_1 and T_1 are the density and temperature at the kinetic layer edge, and n_2, T_2 are the density and temperature at the hydrodynamic layer-plasma bulk interface. Density n_2 and temperature T_2 are determined by the plasma bulk flow and energy balance (see next section). The density n_1 and temperature T_1 are determined by solution of the problem for the kinetic layer[18]. The system of equations is closed if the equilibrium vapor pressure can be specified that determines the parameters at the Teflon surface. In the case of Teflon, the equilibrium pressure formula is used [1]:

$$P = P_c\exp(-T_c/T_s) = n_skT_s \quad (3)$$

where P is the equilibrium pressure, $P_c = 1.84\times10^{20}$ N/m^2 and $T_c = 20815$ K are the characteristic pressure and temperature, respectively.

2.3. Quasi-neutral plasma bulk

The schematic geometry of the thruster is shown in Fig. 1. Several simplifications are made in order to make it possible to develop a simple model. For instance, the anode spike is assumed to a cylinder as shown in Fig. 1. In the present model we assume that all parameters vary in the axial

direction, x (see Fig. 1), but are uniform in the radial direction. The axial component of the mass and momentum conservation equations reads:

$$A(\partial\rho/\partial t + \partial(\rho V)/\partial x) = 2\pi R_2 \Gamma(t,x) \quad (4)$$

$$\rho(\partial V/\partial t + V\partial V/\partial x) = -\partial P/\partial x \quad (5)$$

where A is the cross section of the Teflon chamber ($A=\pi(R_2^2-R_1^2)$), ρ is the plasma density, P is the pressure, V is the plasma velocity, $\Gamma(t,x)$ is the local instantaneous ablation rate, R_2 is the Teflon chamber radius and R_1 is the radius of the spike (see Fig. 1).

The energy transfer from the plasma column to the wall of the Teflon cavity consists of the heat transfer by particle fluxes and radiation heat transfer. In this case, the energy balance equation can be written in the form[15]:

$$\frac{3}{2} n_e (\partial T_e/\partial t + V\partial T_p/\partial x) = Q_J - Q_r - Q_F \quad (6)$$

where T_e is the electron temperature, Q_J is the Joule heat, Q_r is the radiation heat and Q_F is the particle flux. The radiation energy flux Q_r includes the radiation in a continuum spectrum based on a theoretical model[20]. The Joule heat source is assumed to be concentrated in the pinch region by the abode tip (see Fig.1). The average current density in this region is used as a parameter of the model. The particle convection flux Q_F includes energy associated with electron and ion fluxes to the dielectric wall that leads to plasma cooling. Our estimations and previous calculation show[21] that the electron temperature varies only slightly with axial position and therefore we performed the calculation assuming $\partial T_e/\partial x=0$.

The temperature inside the Teflon wall can be calculated from the heat transfer equation:

$$\partial T/\partial t = a\partial^2 T/\partial r^2 \quad (7)$$

where a is the thermal diffusivity. This is the one-dimensional equation in the radial direction. This assumption can be made since the heat layer thickness near the surface is smaller than the Teflon cylinder curvature R_2 and also less than the characteristic length of plasma parameter changes in the axial direction. In order to solve this equation, we use the following boundary and initial conditions[15]:

$$\begin{aligned} &-\lambda\partial T/\partial x(x=0) = q(t) - \Delta H\cdot\Gamma - C_p(T_s-T_o)\,\Gamma \\ &\lambda\partial T/\partial x(x=\infty) = 0 \quad (8) \\ &T(t=0)=T_o \end{aligned}$$

where x=0 corresponds to the inner dielectric surface, ΔH is the ablation heat, Γ is the rate of Teflon ablation per unit area, T_o is the initial room temperature and q(t) is the density of the heat flux, consisting of the radiative and particle convection fluxes, and T_s is the Teflon surface temperature. The solution of this equation is considered for two limiting cases of substantial and small ablation rate very similar to that described in Ref. 15.

Having calculated the plasma density and electron temperature, we calculate the chemical plasma composition considering Local Thermodynamic Equilibrium (LTE) in the way described previously[15,22,23]. In the considered range of electron temperature (1-4 eV) and plasma density (10^{22}-10^{24} m^{-3}) we will assume that polyatomic Teflon molecules C_2F_4 fully dissociate and we will start our consideration from the point when we have gas containing C and F. The Saha

equations for each species (C and F) are supplemented by the conservation of nuclei and quasi-neutrality.

In the present model we use the experimental current waveform as an input condition. We assume that the pulse energy is supplied by a simple LRC circuit with fixed elements. In this case, the current produced by an underdamped LRC circuit can be approximated as:

$$I(t) = I_p \cdot \sin(\alpha t)\exp(-\beta t) \quad (9)$$

where $I_p = \sqrt{\frac{2E}{L}}$; $\alpha = \sqrt{\frac{1}{LC}}$; $\beta = \frac{R}{2L}$; L is the effective inductance in the circuit, C is the capacitance, R is the total circuit resistance, and E is the pulse energy. The best fit with the experimental waveform (frequency) corresponds to $\alpha = 0.9 \cdot 10^6\ s^{-1}$. For C=33. 6 μF we can estimate that L in the circuit is about $3.7 \cdot 10^{-8}$ H. For an energy of 67 J, the amplitude of the current waveform I_p equals $6 \cdot 10^4$ A.

The current waveform was measured for AZ PPT-3 using an integrated Rogowski coil. The data that were taken for AZ-PPT3 fired at 25, 50 and 67J with the 33.6 microF capacitor are shown in Fig. 2. It can be seen that the thruster exhibits damped sinusoidal behavior typical of ablative pulsed plasma thruster. The measurement technique was the same as described in Ref. 11. The current waveform is used as an input parameter in our model.

It was estimated above that under the conditions considered, the current is fully pinched during the main part of the discharge. The current is concentrated between the anode tip end and the cathode as schematically shown in Fig. 1. In general, the current density distribution in that pinched area is two-dimensional and can be calculated using the magnetic transport equation.

However, in the framework of the present 1D model of the plasma flow, only the average current density is considered. The current density peaks at the anode spike tip, $j_a=I/\pi R_1^2$ and then decreases toward the cathode. In the present work we use the current density as a parameter in the range $(0.2 - 1)\, j_a$.

3. Results

In this section we present results of calculation of the plasma parameters during the discharge pulse for the AZ-PPT. As a working example, we consider AZ-PPT-3 as it shows the best device performance. This thruster has a Teflon chamber length of 57 mm, the radius of the Teflon R_2=12.5 or 19 mm, and the radius of the anode spike R_1~6 mm. The simulations are performed assuming a free stream condition at the thruster exit, e.g. the plasma velocity equals the local sound speed at x=L. Based on the calculated plasma parameter distribution, we calculate the thruster performance characteristics, such as mass ablated during the pulse, average specific impulse, and gasdynamic impulse bit.

The plasma density spatial and temporal distribution is shown in Fig. 3. The plasma density peaks at about $8\cdot10^{23}$ m^{-3} at 3 μs that corresponds to the first current peak. One can see also that the plasma density decreases towards the cathode (along x) as a result of the plasma acceleration. At the exit plane, the plasma density is about 60% of the plasma density near the anode base (x=0).

The electron temperature temporal variation is shown in Fig. 4 with discharge energy as a parameter. The electron temperature peaks at 3.7 eV in the case of 50 J and at 4.3 eV in the case of 75 J at about 1.5 μs. The electron temperature oscillations correspond to the discharge current oscillation shown above.

As a result of the oscillations in electron temperature and plasma density, the ionization degree calculated assuming LTE also oscillates as shown in Fig. 5. Initially, during the first current peak, the plasma is strongly ionized and the thruster produces a plume containing mainly C and F ions and electrons. At late time, the ionization degree at the peaks is about 0.5. This means that toward the pulse end the thruster produces a large amount of neutrals.

The calculated thruster performance characteristics integrated over the 15 μs pulse are shown in Fig. 6. Here we show an example of performance calculation for AZ-PPT 3 firing at 25 J. For comparison a parameter range measured experimentally is also shown. The impulse bit and mass bit strongly increase with parameter α, which is a measure of the current density in the pinched region. One can see that all measured parameters agree with our model predictions when the parameter $\alpha \approx 0.55$. This result suggests that even though the current is focused at the anode tip, the average current density in the pinched area is smaller than that at the anode. The effect of varying the Teflon chamber inner diameter ($2R_2$, see Fig. 1) is shown in Fig. 7. One can see that the model predicts a decrease of impulse bit with the increasing propellant inner diameter (ID) in agreement with experiment.

The calculation of the AZ-PPT-3 performance for the case of high pulse energy is shown in Fig.8. One can see that in this case, agreement with the experiment occurs when $\alpha \approx 0.7$-0.8. This means that in the case of the high pulse energy, the average current density is higher and closer to the anode current density. This is an expected result that means that in the case of higher pulse energy (higher current) the current is more constricted near the anode tip. The effect of the pulse energy on the thrust-to–power ratio is shown in Fig. 9 where pulse energy is used as a parameter. It can be seen that the thrust-to–power ratio decreases with the energy for the constant parameter α.

However, since in the experiment (Ref. 11) it was obtained that the thrust-to–power ratio actually increases with energy one can conclude that the parameter α must be higher in the case of high energy. Thus the comparison of the model prediction with experimental data suggests that the pinch effect increase with the pulse energy.

The simulated results are summarized in Fig. 10 where the dependence of the parameter α (average current density to the current density at the anode tip ratio) for which the agreement with the measured impulse bit was obtained is shown as a function of the pulse energy. Here also the Teflon chamber inner diameter (ID) is used as a parameter. Generally it can be seen that the average current density increases with the pulse energy as was mentioned above. An interesting result is the dependence of the average current density on the Teflon chamber ID. One can see that the average current density more significantly increases in the case of the large propellant ID. This observation can be explained as follows. When the propellant ID is larger, the model predicts that the plasma density in the channel is smaller. Therefore one can expect higher current density in the case of larger propellant ID since, in the pinched area, the current constriction is limited by the plasma pressure.

Taking into account that the average current density varies with the pulse energy, the dependence of the thrust-to-power ratio (T/P) on the Teflon chamber length L was calculated. These results are shown in Fig. 11. One can see that T/P much higher in the case of the smaller propellant ID. Also, in this case the T/P variation with the energy pulse is relatively moderate. In the case of the large propellant ID, T/P significantly increases with the pulse energy. In all cases there is an optimal length corresponded to the maximal T/P. In the case of 1" ID propellant the maximal T/P is predicted to be at L~40 mm, while in the 1.5" ID propellant case it corresponds to L~50 mm. After the maximum the T/P significantly decreases with L, especially in the case of smaller ID. In

this study we fix the length of the pinched area meaning that when the Teflon chamber length L increases the anode spike length also increases (see Fig. 1). As result the length of the pinched area normalized by the total length of the propellant decreases and therefore the plasma in the channel is less heated. This is the main reason why T/P decreases when L is high.

4. Summary

In this paper a model of the discharge in the recently developed Ablative Z-pinch Pulsed Plasma Thruster is presented. This device utilizes the pinch effect to produce an axially streaming plasma. The model includes Joule heating of the plasma, heat transfer to the Teflon, and Teflon ablation kinetics. Mechanisms of energy transfer from the plasma column to the propellant bar include heat transfer by particle convection and by radiation. In addition it was assumed that the current is fully pinched near the anode tip during the main part of the discharge. The average current density in the pinched area is used as a parameter of the problem. The model predicts that the electron temperature peaks at about 4 eV and the plasma density peaks at about $8 \cdot 10^{23}$ m^{-3}. During the initial stage of the discharge, plasma is predicted to be strongly ionized, while at the late time the ionization degree peaks at about 0.5. Thruster performance characteristics such as impulse bit, specific impulse, and the mass bit were calculated. In the case of low pulse energy, all measured thruster performance characteristics agree with our model predictions when the average current density to anode current density ratio α is about 0.55. In the case of high pulse energy, similar agreement with experiment occurs when $\alpha \approx 0.7$-0.8. This means that in the case of higher pulse energy (higher current) the current is more constricted near the anode tip. The model also predicts that the impulse bit decreases with increasing propellant inner diameter (ID) in agreement with experiment. The comparison of the model prediction with experimental data suggests that the pinch effect and the thrust-to-power ratio increase with pulse energy. It was

predicted that the thrust-to-power ratio dependence on the Teflon chamber length has a maximum. The non-monotonic behavior of the T/L with Teflon chamber length is more pronounced in the case of the smaller propellant inner diameter.

Acknowledgements

The authors from University of Michigan gratefully acknowledge the financial support by the Air Force Office of Scientific Research through grant F49620-99-1-0040.

REFERENCES

[1] R. L. Burton and P. J. Turchi, "Pulsed plasma thruster", Journal of Propulsion and Power, vol.14, 5, 1998, pp. 716-735

[2] R. J. Vondra, "The MIT Lincoln laboratory pulsed plasma thruster", AIAA Paper 76-998, 1976.

[3] P. J. Turchi, Directions for improving PPT performance, *Proceeding of the 25th International Electric Propulsion Conference*, vol. 1, Worthington, OH, 1998, pp. 251-258.

[4] E. Antonsen, R.L. Burton and F. Rysanek, "Energy measurements in a co-axial electromagnetic pulsed plasma thruster", Paper AIAA-1999-2292.

[5] F. Gulczinski III, M. Dulligan, J. Lakes and G. Spanjers, "Micropropulsion research at AFRL", Paper AIAA-2000-3255

[6] R.L. Burton and S.S. Bushman, "Probe measurements in a Co-axial gasdynamic PPT", *35th Joint Propulsion Conference, Los Angeles, CA, June 1999*, AIAA Paper 99-2288.

[7] F. Rysanek and R.L. Burton, "Effects of geometry and energy on a coaxial Teflon pulsed plasma thruster", *36th Joint Propulsion Conference, Huntsville AL, July 2000*, AIAA Paper 2000-3429.

[8] I.G. Mikellides and P.J. Turchi, "Optimization of pulsed plasma thrusters in rectangular and coaxial geometries", IEPC Paper – 99-211.

[9] K.T. Lee, D.E. Kim and S.H. Kim, "Reversed current structures in a Z-pinch plasma", Phys. Rev. Lett., 85, 2000, 3834.

[10] R.G. Jahn, W. Jaskowsky, and R.L. Burton, "Ejection of a pinched plasma from an axial orifice", AIAA Journal, 3(10), 1965, pp. 1862-1866.

[11] T.E. Markusic, K.A. Polzin, J.Z. Levine, C.A. McLeavey and E.Y. Choueiri, "Ablative Z-Pinch Pulsed Plasma Thruster, AIAA Paper 2000-3257.

[12] G. G. Spanjers, J. S. Lotspeich, K.A. McFall, and R. A. Spores, Propellant losses because of particulate emission in a pulsed plasma thruster, *Journal of Propulsion and Power*, Vol. 14, 4, 1998, pp. 554-559.

[13] M. Keidar, I. D. Boyd and I.I. Beilis, "Model of particulate interaction with plasma in a Teflon Pulsed Plasma Thruster", J. Prop. Power, 17, No. 1, 2001, pp. 125-131.

[14] M. Keidar and I.D. Boyd, "Device and plume model of an electrothermal pulsed plasma thruster", Paper AIAA-2000-3430.

[15] M. Keidar, I.D. Boyd and I.I. Beilis, "Electrical discharge in the Teflon cavity of a coaxial pulsed plasma thruster', IEEE Trans. Plasma Sci., 28, 2000, p. 376-385.

[16] M. Keidar, I.D. Boyd and I.I. Beilis, "On the model of Teflon ablation in an ablation-controlled discharge", J. Phys. D: Appl. Phys., 34, June, 2001, pp. 1675-1677.

[17] N. A. Krall and A.W. Trivelpiece, Principles of Plasma Physics, McGraw-Hill, New York, 1973.

[18] M. Keidar, J. Fan, I.D. Boyd and I.I. Beilis, "Vaporization of heated materials into discharge plasmas", J. Appl. Phys., 89, 2001, pp. 3095-3099.

[19] I.I. Beilis, "Parameters of the kinetic layer of arc discharge cathode region", IEEE Trans. Plasma Sci.,1985, PS-13, p. 288-290.

[20] G. I. Kozlov, V. A. Kuznetsov, and V. A. Masyukov, "Radiative losses by argon plasma and the emissive model of a continuos optical discharge", Sov. Phys. JETP, 39, 1974, pp.463-468.

[21] P. Kovatya and J. J. Lowke, "Theoretical prediction of ablation stabilised arcs confined in cylindrical tubes", J. Phys. D: Appl. Phys., 17, 1984, pp. 1197-1212.

[22] P. Kovatya, "Thermodynamic and transport properties of ablated vapors of PTFE, alumina, perspex and PVC in the temperature range 5000-30000 K", IEEE Trans. Plasma Sci., 12, 1984 pp. 38-42.

[23] C.S. Schmahl and P.J. Turchi, , "Development of equation-of-state and transport properties for molecular plasmas in pulsed plasma thrusters. Part I: A two-temperature equation of state for Teflon", Proc. Inter. Electr. Propul. Conf. Pp. 781-788, 1997.

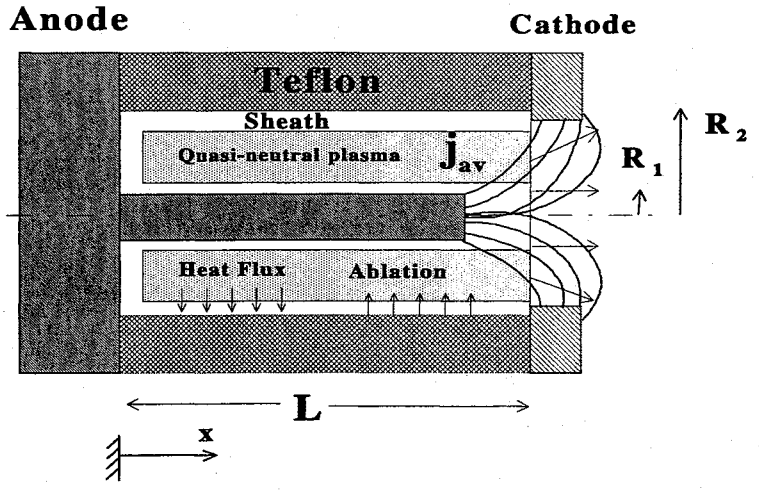

Figure 1. *Schematic of the simplified AZPPT geometry adopted in the model*

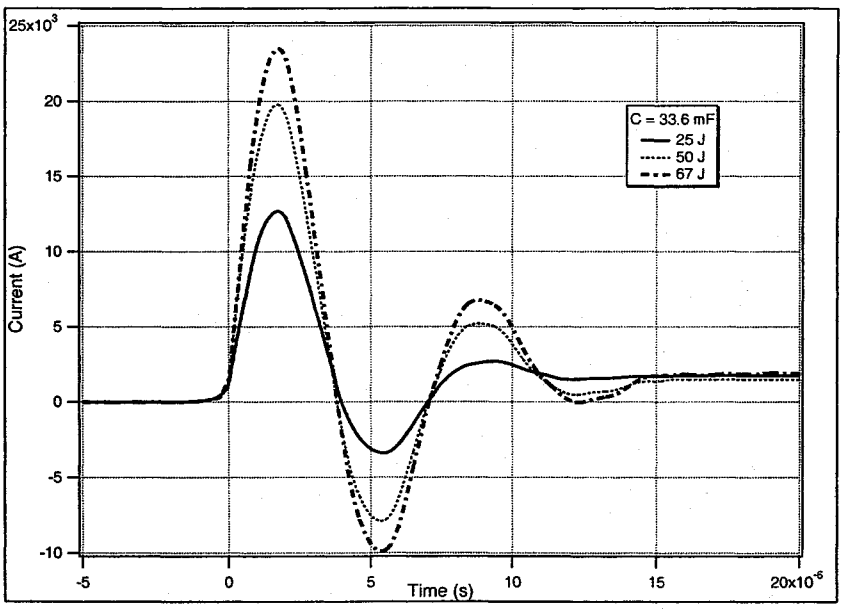

Figure 2. *AZ-PPT-3 current waveform*

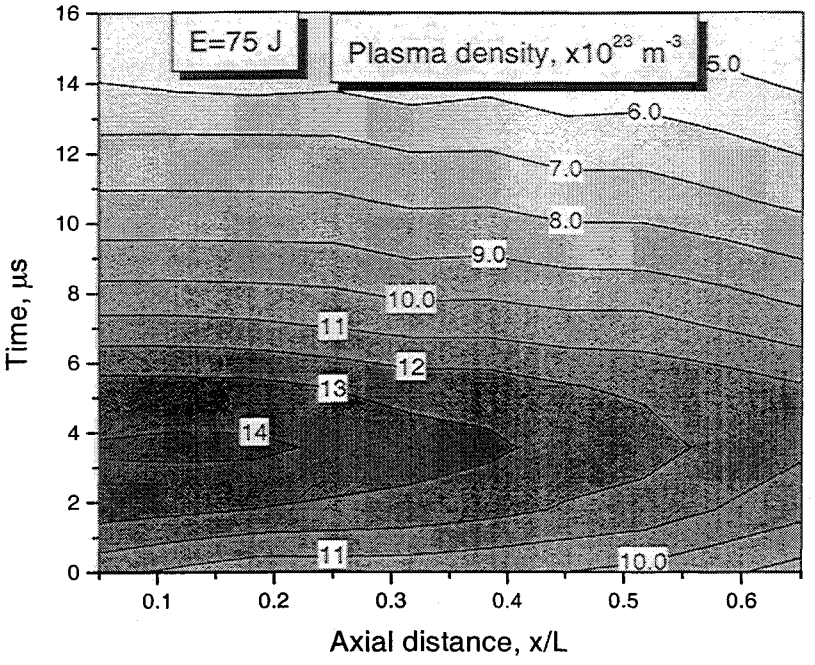

Figure 3. *Plasma density temporal and axial (along channel centerline) variation during the pulse.*

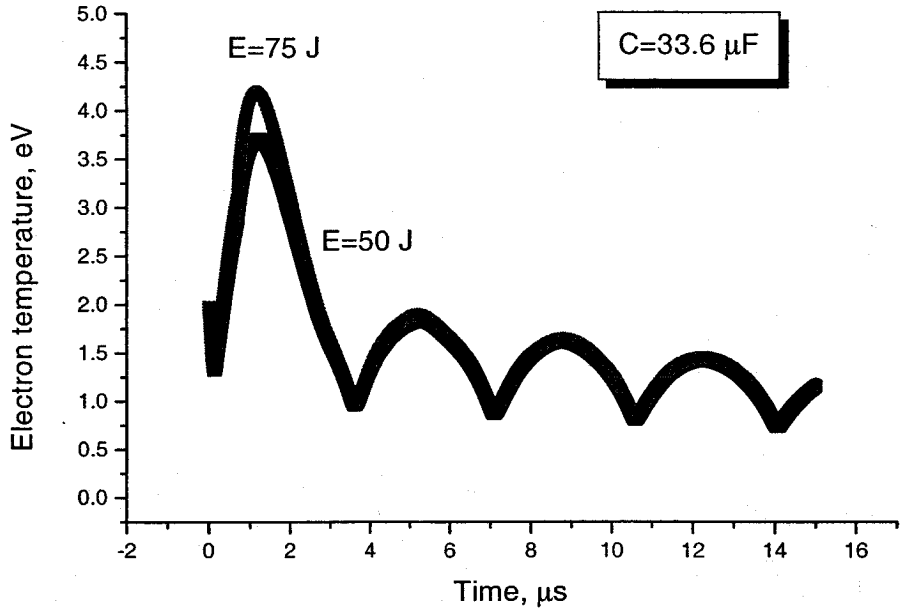

Figure 4. *Electron temperature temporal variation during the pulse with the pulse energy as a parameter*

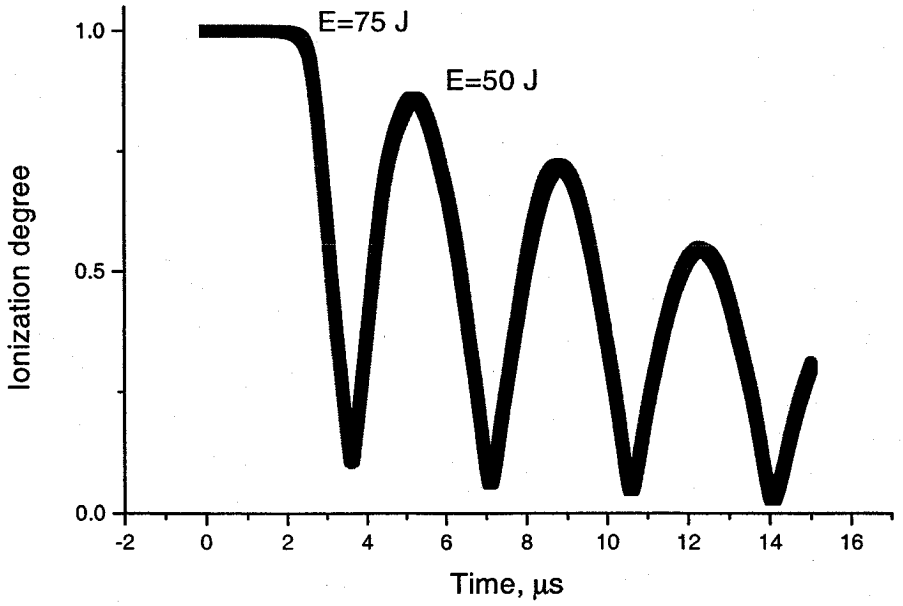

Figure 5. *Ionization degree temporal variation during the pulse*

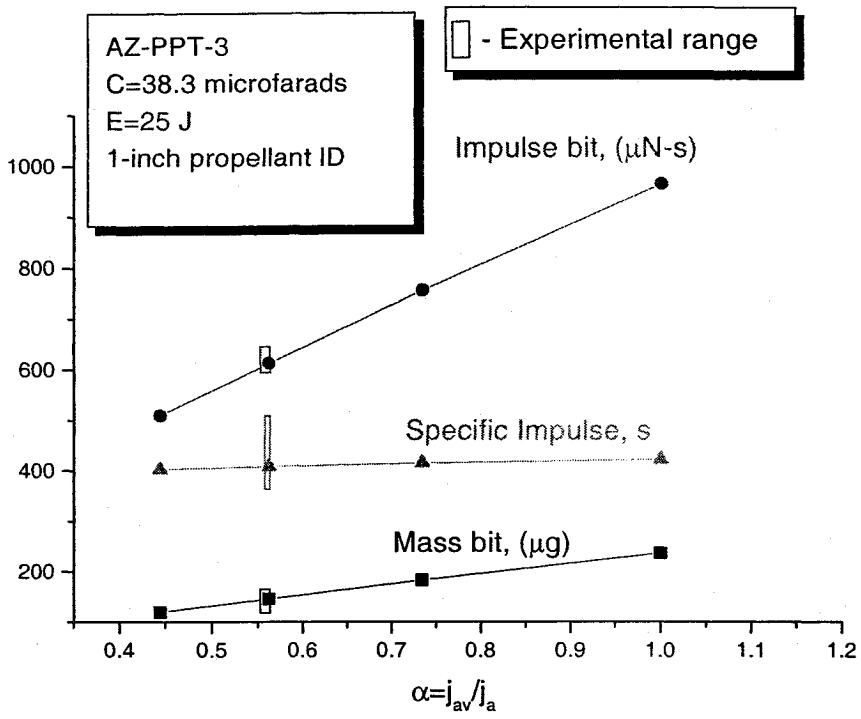

Figure 6. *AZ-PPT-3 performances as a function of average current density to the anode current density ratio and comparison with experiment*

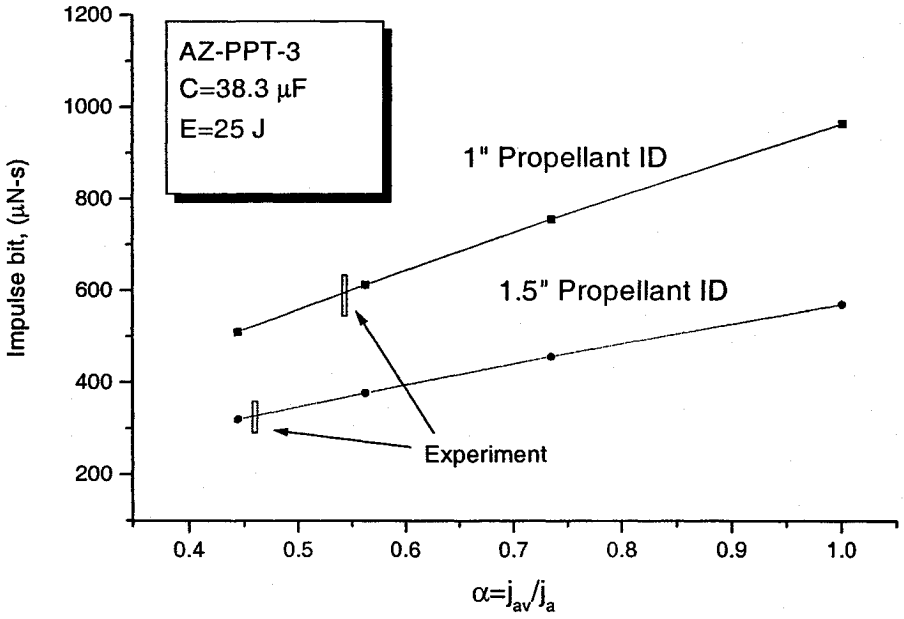

Figure 7. *AZ-PPT-3 impulse bit as a function of average current density to the anode current density ratio with propellant ID ($2R_2$) as a parameter*

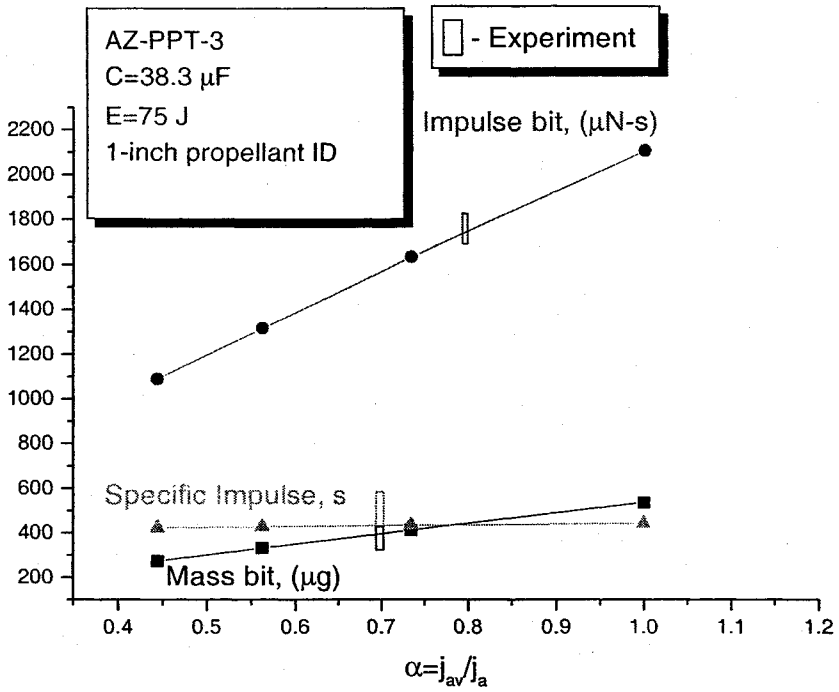

Figure 8. *AZ-PPT-3 performances as a function of average current density to the anode current density ratio and comparison with experiment*

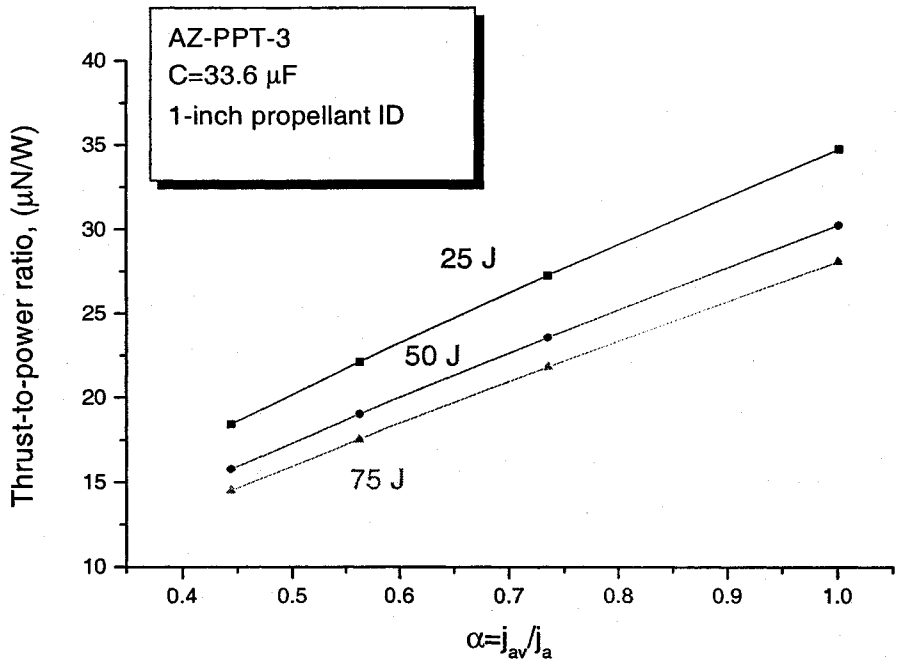

Figure 9. *Thrust-to-power ratio as a function of average current density to the anode current density ratio with pulse energy as a parameter*

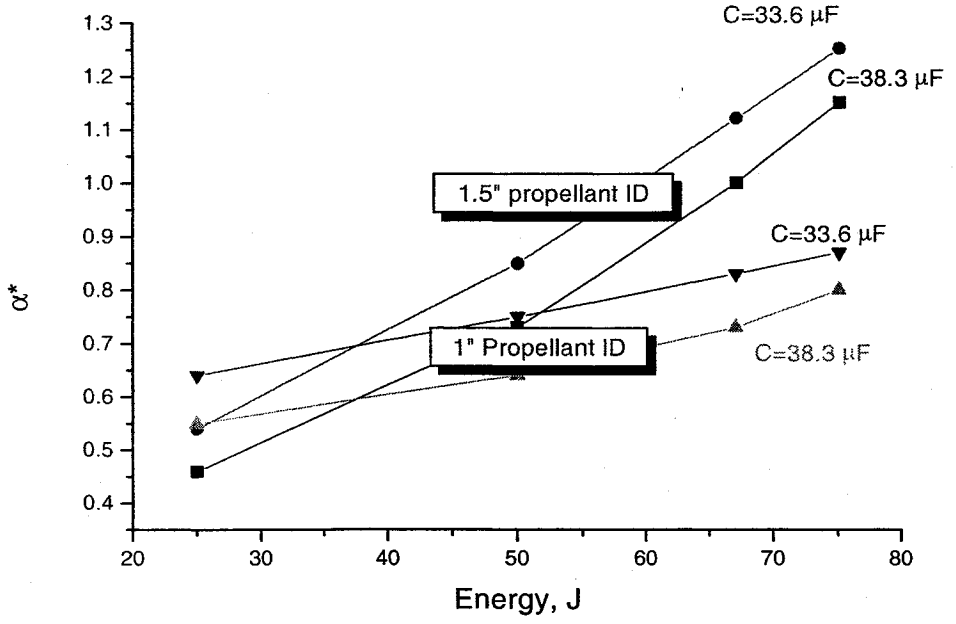

Figure 10. *Average current density to the anode current density ratio α* for which the model agree with experiment as a function of the pulse energy with capacitance and propellant ID as parameters*

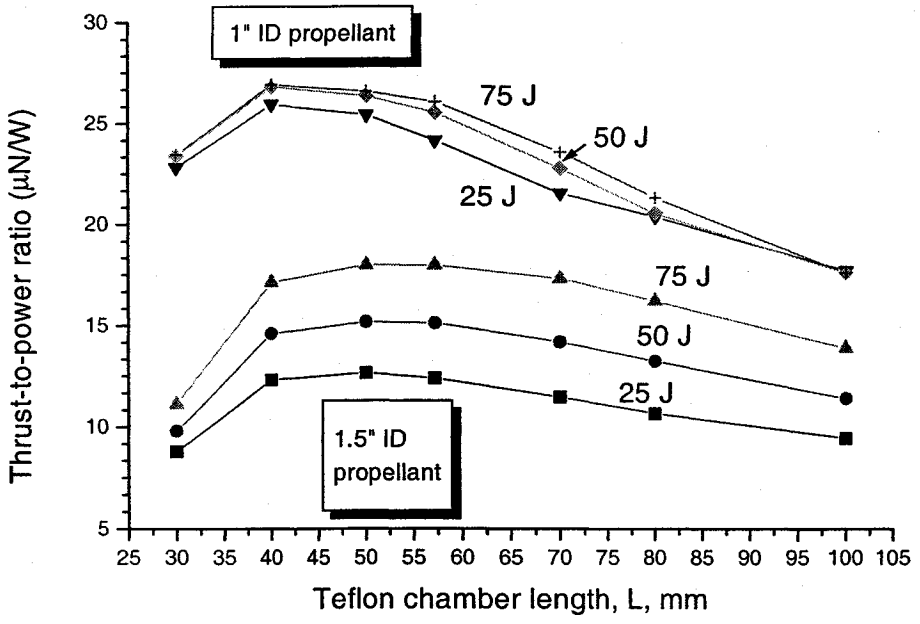

Figure 11. *Thrust-to-power ratio as a function of the Teflon chamber length with pulse energy and the propellant ID as parameters. C=38.3 μF.*